Effect of Protein Incorporation on Nanostructure of the Bicontinuous Microemulsion Phase of Winsor-III Systems: A Small-Angle Neutron Scattering Study (Supporting Information)

Douglas G. Hayes[1,], Javier A. Gomez del Rio[1,2], Ran Ye[1], Volker S. Urban[3], Sai Venkatesh Pingali[3], and Hugh M. O'Neill[3]*

[1] Department of Biosystems Engineering and Soil Science, University of Tennessee, Knoxville, TN 37996-4531 USA, [2] deceased, [3] Biology & Soft Matter Division, Oak Ridge National Laboratory, P.O. Box 2008, Oak Ridge, TN 37831; *To whom all correspondences should be addressed (dhayes1@utk.edu; tel 865-974-7991; fax 865-974-4514)

Langmuir la-2014-0406.R1

Nomenclature

A	Scaling constant (Eq. S10)
AOT	The surfactant Aerosol-OT
a_2	Coefficient of Teubner-Strey SANS function (Eq. S1, *cm*)
a_s	Surface area per surfactant, $Å^2$ (Eq. 1)
b	SANS incoherent background (cm^{-1})
$B\mu E$	Bicontinuous microemulsion
BSA	Bovine serum albumin
C_{bulk}	Constant (Eqs. S11 and S13, $Å^{-5}$)
C_{film}	Constant (Eqs. S12 and S14, $Å^{-3}$)
c_1	Coefficient of Teubner-Strey SANS function (Eq. S1, $cm\ Å^2$)
c_2	Coefficient of Teubner-Strey SANS function (Eq. S1, $cm\ Å^4$)
$CK\text{-}2,13\text{-}E_j$	The alkyl ethoxylate "cyclic ketal surfactant, O-[(2-tridecyl, 2-ethyl-1,3-dioxolan-4-yl) methoxy]–O-methoxy poly(ethylene glycol)$_j$ (j = 5.6 [average] or 3)
d	Quasi-periodic repeat distance (Eq. S3; $Å$)
d_{max}	Average film-to-film distance in BμEs ($Å$)
f_a	Amphiphilicity factor (Eq. S4)
$f_{p,mid}$	The fraction of protein that partitions to the middle (BμE) phase
$f(Q)$	Excess scattering (film contrast, Eq. S10)
I	Scattered intensity (cm^{-1})
I_0	Scattered intensity as $Q \rightarrow 0$ (Eq. S9; cm^{-1})
k_B	Boltzmann's Constant ($J\ K^{-1}$)

l_s	Surfactant monolayer thickness (Eq. S8, $\AA$)
$[P]_{aq}$	Protein concentration of aqueous phase used to prepare W_{III} systems ($g\ L^{-1}$)
$P(Q)$	SANS form factor
Q	Momentum transfer (scattering vector; $\AA^{-1}$)
Q_{max}	maximum Q value ($\AA^{-1}$)
SANS	Small-Angle Neutron Scattering
$S(Q)$	SANS structure factor
S/V	Surface area per volume (for $B\mu Es$; $\AA^{-1}$)
T	Temperature (absolute scale, K)
t	Film thickness (Eqs. S11 and S13; $\AA$)
t_e	Effective film thickness (Eqs. S11 and S12; $\AA$)
T-S	Teubner-Strey SANS function
W_{III}	Winsor-III μE system
Z	Schulz distribution parameter for distribution of Q_{max} (Eq. S10)
α	Oil mass fraction (surfactant and protein-free basis)
δ_1	Mass fraction of AOT among the surfactants
δ_2	Mass fraction of CK-2,13-E_3 among the surfactants
γ	Mass fraction of surfactants
ϕ_i	Volume fraction of phase i
κ_{SANS}	Renormalized bending modulus (Eq. S6; J)
κ_{theor}	Bare bending modulus, theoretical estimate (Eq. S8; J)
μE	Microemulsion
ρ	Scattering length density ($\AA^{-2}$)

ξ	Correlation length (Eq. S2; $\AA$)
ξ_{OZ}	Ornstein-Zernicke correlation length (Eq. S9; $\AA$)

Subscripts

aq	(initial) aqueous phase
bot	bottom phase
mid	middle phase
o	oil
Porod	via modified Porod equation (Eq. S11)
s	surfactant
w	water

Molecular structure of CK-2,13 surfactant

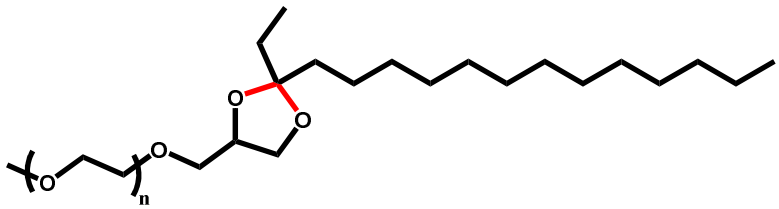

Figure S1. Chemical structure of CK-2,13-O-E_n, *O*-[(2-tridecyl, 2-ethyl-1,3-dioxolan-4-yl) methoxy] –*O*'-methoxy poly(ethylene glycol). Its cleavable bonds are indicated with red.

Volume Fractions and Surfactant Partitioning Between the Three Winsor-III Phases (*System 2a*)

Table S1. Effect of proteins on volume fraction and distribution of surfactant among the three Winsor-III phases for Water/AOT/CK-2,13-$E_{5.6}$/Heptane (*System 2a*), 25°C (bulk contrast) [1,2]

Protein	$[P]_{aq}$, g L^{-1}	ϕ_{bot}	ϕ_{mid}	ϕ_{top}	$f_{AOT,bot}$ [3]	$f_{AOT,mid}$ [3]	$f_{AOT,top}$ [3]	$f_{CK,bot}$ [3]	$f_{CK,mid}$ [3]	$f_{CK,top}$ [3]
No Protein		0.39±0.03	0.32±0.04	0.29±0.03	0.11	0.89	0.00	0.04	0.84	0.12
BSA [4]	1	0.38±0.02	0.22±0.02	0.40±0.00	0.09	0.91	0.00	0.04	0.78	0.18
BSA [4]	0.5	0.37±0.02	0.26±0.03	0.37±0.03	0.09	0.91	0.00	0.04	0.81	0.15
Catalase	1	0.36±0.03	0.35±0.03	0.29±0.02	0.13	0.87	0.00	0.04	0.82	0.14
α-Chymotrypsin	1	0.37±0.04	0.30±0.03	0.32±0.02	0.11	0.89	0.00	0.04	0.77	0.19
Chymotrypsin	0.5	0.35±0.04	0.33±0.02	0.32±0.02	0.13	0.87	0.00	0.04	0.82	0.14
Cytochrome C	1.5	0.38±0.01	0.21±0.02	0.41±0.02	0.08	0.92	0.00	0.04	0.82	0.14
Cytochrome C	1	0.38±0.03	0.22±0.03	0.40±0.03	0.12	0.88	0.00	*0.04*	0.80	0.16
Cytochrome C	0.5	0.37±0.03	0.31±0.03	0.32±0.02	0.13	0.87	0.00	0.04	0.80	0.15
Lysozyme	1.5	0.38±0.01	0.23±0.04	0.39±0.03	0.12	0.88	0.00	0.04	0.80	0.16
Lysozyme	1	0.32±0.01	0.34±0.03	0.34±0.04	0.14	0.86	0.00	0.04	0.82	0.15
Lysozyme	0.5	0.32±0.01	0.36±0.02	0.32±0.02	0.15	0.85	0.00	0.04	0.82	0.14
Ovalbumin	1	0.35±0.01	0.33±0.01	0.32±0.01	0.13	0.87	0.00	0.04	0.79	0.18
Pepsin	2	0.34±0.01	0.37±0.02	0.29±0.02	0.12	0.88	0.00	0.04	0.77	0.19
Ribonuclease	0.5	0.34±0.02	0.35±0.01	0.31±0.02	0.13	0.87	0.00	0.04	0.79	0.17

[1] Compositional information for the Winsor-III (W_{III}) system is given in Table 1; [2] Column headings: $[P]_{aq}$ = concentration of protein in aqueous solutions used to form W_{III} system; ϕ_j = volume fraction of phase j, $f_{i,j}$ = fraction of component i residing in phase j; subscripts *AOT*, and *CK* refer to Aerosol-OT, and CK-2,13-$E_{5.6}$, respectively; subscripts *bot*, *mid*, and *top* refer to bottom, middle and top phases, respectively; [3] $f_{i,j}$ values were obtained from Winsor-III systems that used D_2O, with errors for reported values are within ± 5%; ϕ_j values are the average ± standard deviation for an entire D_2O/H_2O dilution series; [4] bovine serum albumin

Small-Angle Neutron Scattering (SANS) Instrumentation and Sample Information

SANS experiments were conducted using the NG3 30 *m* system at the National Institute of Standards and Technology (NIST), Gaithersburg, MD USA [1] or the Bio-SANS [2] or GP-SANS [3] instrument at Oak Ridge National Laboratory (ORNL), Oak Ridge, TN USA. The incident wavelengths were 5.65 Å, 6.09 Å, and 4.75 Å for the NG3, Bio-SANS, and GP-SANS systems, respectively. Two different detector distances were employed to allow for an effective range for the momentum transfer, Q (= $4\pi\ \lambda^{-1}\sin[\theta/2]$, where θ is the scattering angle and λ is the wavelength of incident neutrons), of 0.006 – 0.50 $Å^{-1}$ and 0.003 –0.50 $Å^{-1}$, for the NIST and ORNL systems, respectively. The sample temperature was set at 25 ± 0.1 °C for all experiments. Sample distribution between the three SANS apparatuses consists of the following. All Water/AOT/CK-2,13-$E_{5.6}$/CK-E_3/*d*-Heptane (*System 1*) W_{III} samples of the (bulk contrast) were analyzed at NIST-NG3. For H_2O+D_2O/AOT/CK-2,13-$E_{5.6}$/Heptane W_{III} (*System 2a*, bulk contrast), the following samples were analyzed using Bio-SANS (concentrations are those or protein in aqueous phase used to form the W_{III} system): no protein, α-chymotrypsin (0.5 g/L_{aq}), BSA (1.0 and 0.5 g/L), cytochrome c (1.5, 1.0, and 0.5 g/L_{aq}), lysozyme (1.5 g/L_{aq}), and pepsin (2.0 g/L_{aq}); and, the following were analyzed using GP-SANS: α-chymotrypsin (1.0 g/L_{aq}), catalase (1.0 g/L_{aq}), lysozyme (1.0 and 0.5 g/L_{aq}), ovalbumin (1.0 g/L_{aq}), and ribonuclease (0.5 g/L_{aq}). All samples for *System 2b* (film contrast) were analyzed using Bio-SANS.

A typical reduction protocol was used to yield normalized scattering intensities, $I(Q)$ (cm^{-1}), as a function of Q ($Å^{-1}$), which consisted of subtracting scattering contributions from the empty cell and background scattering, sorting data collected from the two different detector distances, and subtracting scattering due to the empty cell [4]. Volume fractions for the surfactants were calculated based on densities for AOT and CK-2,13 of 1.14 $g\ mL^{-1}$ [5] and 0.95 $g\ mL^{-1}$ (measured

in the laboratory), respectively. Data reduction was conducted software written by NIST staff scientists that employed Igor Pro (v. 5.0.4.7, WaveMetrics, Lake Oswego, OR USA) as a platform [4].

SANS: Model Fitting to Data *(BμEs)*

For a *bulk contrast*, *I(Q)* vs. *Q* data were fit using the Teubner-Strey (*T-S*) function [6-7]:

$$I(Q) = \frac{1}{a_2 + c_1 Q^2 + c_2 Q^4} + b \tag{S1}$$

where *b* is the incoherent background (determined via Porod analysis, and then subtracted from the data prior to analysis) and a_2, c_1, and c_2 are coefficients employed to calculate the following parameters:

$$\xi = \frac{1}{\sqrt{\frac{1}{2}\sqrt{\frac{a_2}{c_2}} + \frac{c_1}{4c_2}}} \tag{S2}$$

$$d = \frac{2\pi}{\sqrt{\frac{1}{2}\sqrt{\frac{a_2}{c_2}} - \frac{c_1}{4c_2}}} \tag{S3}$$

$$f_a = \frac{c_1}{\sqrt{4a_2c_2}} \tag{S4}$$

where ξ is the correlation length, *d* the quasi-periodic repeat distance (i.e., the distance across aqueous plus oil nanochannels), and f_a the amphiphilicity factor. ξ can be used to determine the surface area per volume, *S/V* [7]:

$$\frac{S}{V} = \frac{4\phi_{w,mid}\phi_{o,mid}}{\xi} \tag{S5}$$

where $\phi_{w,mid}$ and $\phi_{o,mid}$ refer to the volume fraction of water and oil in the middle ($B\mu E$) phase, respectively.

Another parameter that can be obtained from SANS analysis (i.e., from d and ξ) is the renormalized bending modulus, κ_{SANS} [8-11]:

$$\kappa_{SANS} = \frac{5\sqrt{3}}{64} k_B T \frac{2\pi\xi}{d} \quad \text{(S6)}$$

where k_B is Boltzmann's constant and T the absolute temperature. κ_{SANS}, derived from the Gaussian random field model, describes membrane fluctuations up to the characteristic length scale of the $B\mu Es$ (d), and is directly related to both the saddle-splay modulus and the intrinsic bending modulus for the bare surfactant interface[8-11]. κ_{SANS} is also directly related to f_a, easily shown by manipulating Eqs. S2-S4:

$$f_a = \frac{1-\left(\frac{2\pi\xi}{d}\right)^2}{1+\left(\frac{2\pi\xi}{d}\right)^2} \quad \text{(S7)}$$

where the term $2\pi\xi/d$ is directly proportional to κ_{SANS} by Eq. S6. Therefore, the Lifshiz line corresponds to $\xi = d/2\pi$, and $\kappa_{SANS} = 0.1353\ k_BT$ (via Eq. S6). An increase in amphiphilicity corresponds to a decrease in f_a, and therefore an increase in $2\pi\xi/d$ and κ_{SANS}. The theoretical bare bending elasticity constant, κ_{theor}, can be derived via the following equation [8-11]:

$$\frac{\kappa_{theor}}{k_B T} = \frac{\kappa_{SANS}}{k_B T} + \frac{3}{4\pi} \ln\left(\frac{d}{2l_s}\right) \quad \text{(S8)}$$

where l_s is the thickness of the surfactant monolayer. Eq. S8 incorporates a renormalization contribution as a correction to Eq. S6. Similar to κ_{SANS}, an increase of κ_{theor} is attributable to an increase of surfactant efficiency and decrease of thermal fluctuations [8-11]. κ_{theor} provides

reasonably close estimates to bending constant values provided by neutron spin-echo techniques [8-11].

For the *film contrast*, the following scattering function is employed, which refers to Ornstein-Zernicke form of critical scattering (Eq. S1, $c_2 = 0$) [7]:

$$I(Q) = f(Q)\frac{I_0}{1+\xi_{OZ}^2 Q^2} + b \qquad \text{(S9)}$$

where $I_0 = a_2^{-1}$ and $\xi_{oz} = (c_1/a_2)^{0.5}$. The latter is referred to as the Ornstein-Zernicke correlation length. The term $f(Q)$ is associated with a faint peak of excess scattering, which is described by a normalized form of the Schulz distribution[7]:

$$f(Q) = A\left(\frac{Z+1}{Q_{\max}}\right)^{Z+1}\frac{Q^Z}{\Gamma(Z+1)}\exp\left(-\frac{(Z+1)Q}{Q_{\max}}\right) \qquad \text{(S10)}$$

where A is a scaling constant and Z a parameter of the distribution. Q_{max} provides the average film-to-film separation in $B\mu Es$, d_{max} ($2\pi / Q_{max}$). The polydispersity of Q_{max} via the Schulz distribution ($\sigma / Q_{\max}$) equals $(Z+1)^{-0.5}$.

In the Porod regime (large Q), the following "modified Porod" equations were employed for bulk and film contrast data, respectively [7]:

$$I(Q) = C_{bulk}Q^{-4}\exp\left(-t^2Q^2\right) + b \qquad \text{(S11)}$$

$$I(Q) = C_{film}Q^{-2}\exp\left(-t^2Q^2\right) + b \qquad \text{(S12)}$$

where:

$$C_{bulk} = 2\pi(\Delta\rho)^2\frac{S}{V_{Porod}} \qquad \text{(S13)}$$

$$C_{film} = 2\pi(\Delta\rho)^2\left(\frac{S}{V_{Porod}}\right)^{-1}\phi_{s,mid}^2 \qquad \text{(S14)}$$

The parameters $(\Delta\rho)^2$ and *S/V* refer to the difference in scattering length density squared (i.e., the neutron contrast) and specific surface area per volume of the $B\mu E$ phase, respectively. The effective thickness of the interface, t_e ($\approx l_s$), is determined from *t*: $t_e = \sqrt{2\pi t^2}$.

Effect of Proteins on Middle, Bicontinuous Microemulsion (BμE), Phase of W_{III}: AOT/CK-2,13-$E_{5.6}$ System (*Bulk Contrast*)

Determination of Teubner-Strey Parameters

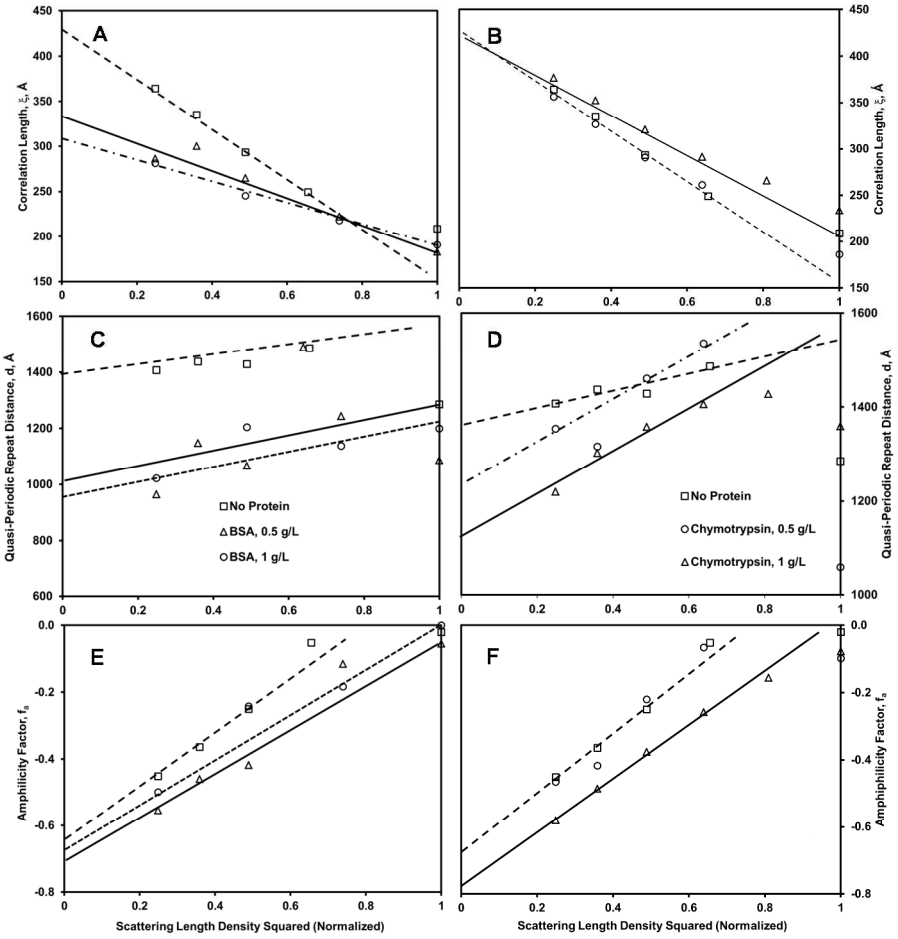

Figure S2. Effect of scattering length density squared, $(\Delta\rho)^2$, on values for parameters derived from the *T-S* function (Eqs. S1-S4) of the H_2O+D_2O /AOT /CK2,13-$E_{5.6}$ /Heptane Winsor-III (W_{III}) bicontinuous microemulsion ($B\mu E$) phase at 25°C (*System 2a*; bulk contrast), containing **(A,C,E)** BSA and **(B,D,F)** α-chymotrypsin at the given aqueous phase concentrations. Compositional information for the W_{III} system is given in Table 1 of the main paper. Values of ξ, d, and f_a were obtained by extrapolating to $(\Delta\rho)^2$=0. Chymotrypsin (1.0 g/L_{aq}) samples were analyzed via the GP-SANS apparatus, while all others were analyzed via Bio-SANS.

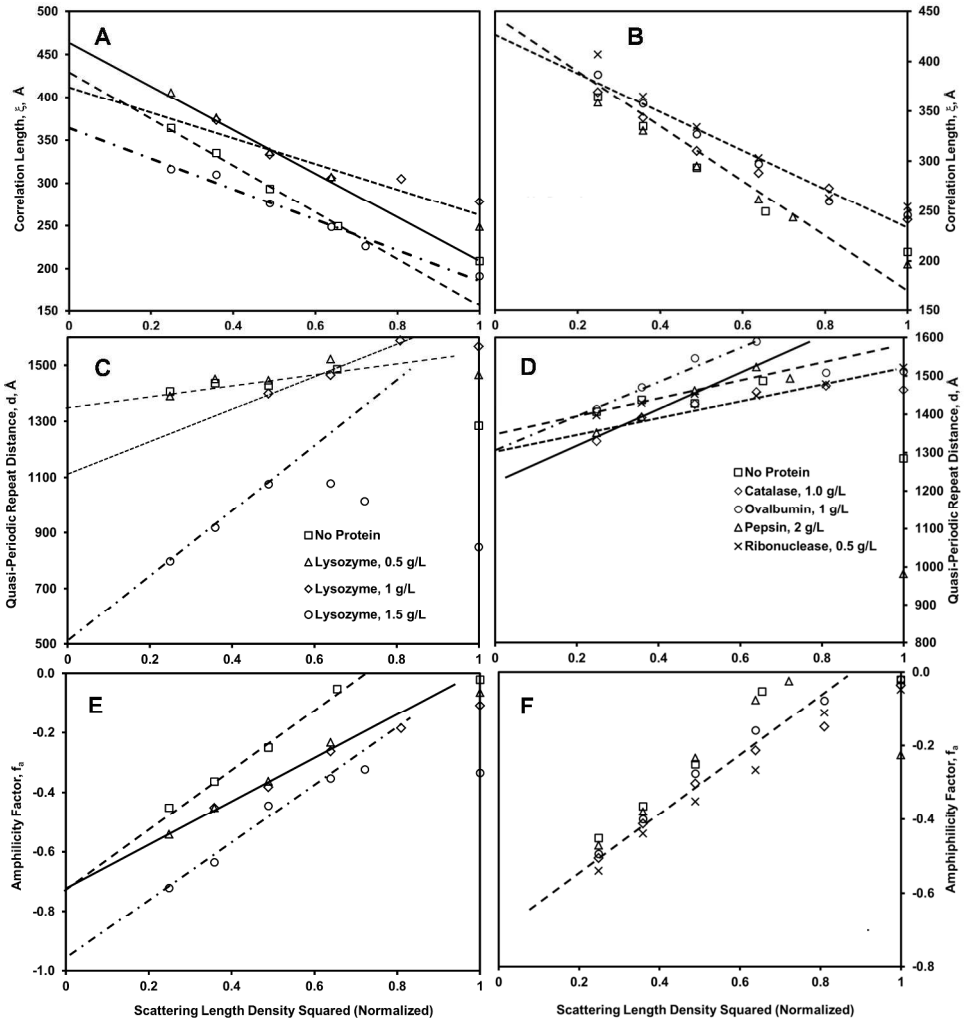

Figure S3. Effect of scattering length density squared, $(\Delta\rho)^2$, on values for parameters derived from the *T*-*S* function (Eqs. S1-S4) of the H_2O+D_2O /AOT /CK2,13-$E_{5.6}$ /Heptane Winsor-III (W_{III}) bicontinuous microemulsion ($B\mu E$) phase at 25°C (*System 2a*; bulk contrast), containing **(A,C,E)** lysozyme, and **(B,D,F)** catalase, ovalbumin, pepsin, and ribonuclease at the given aqueous phase concentrations. Compositional information for the W_{III} system is given in Table 1 of the main paper. Values of ξ, d, and f_a were obtained by extrapolating to $(\Delta\rho)^2$=0. Lysozyme (1.0 g/L_{aq}) samples were analyzed via the GP-SANS apparatus, while all others were analyzed via Bio-SANS. Lysozyme (1.5 g/L_{aq}) and pepsin (2.0 g/L_{aq}) samples were analyzed via the Bio-SANS apparatus, while all others were analyzed via GP-SANS.

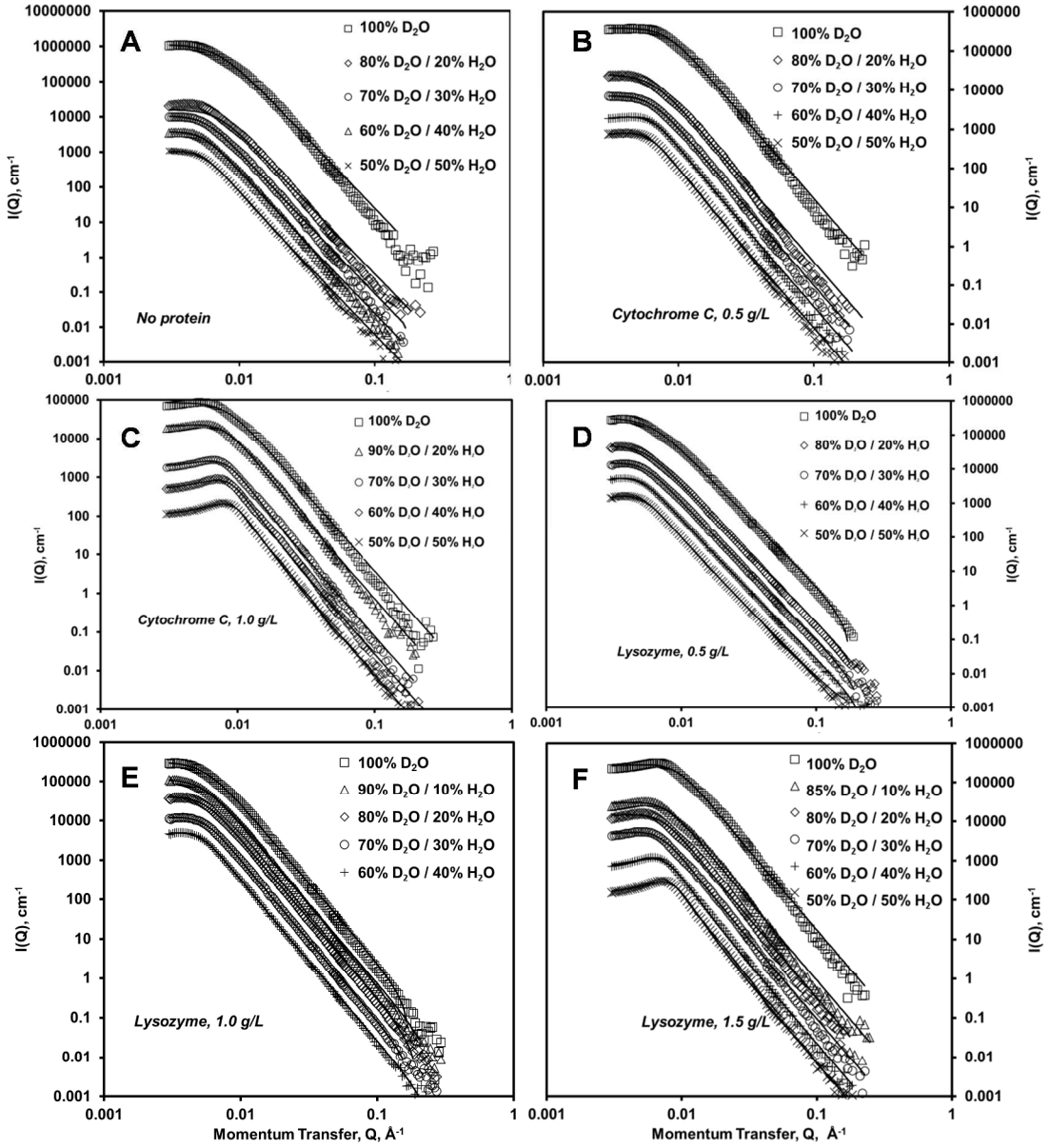

Figure S4. SANS data for the BμE phase of the H_2O+D_2O /AOT /CK2,13-$E_{5.6}$ /Heptane Winsor-III (W_{III}) bicontinuous microemulsion ($B\mu E$) phase at 25°C (*System 2a*; bulk contrast), containing **(A)** no protein, **(B,C)** cytochrome C (0.5 and 1.0 g/L_{aq}), and **(D-F)** lysozyme (0.5, 1.0, and 1.5 *g/L*) as a function of the H_2O / D_2O ratio. Compositional information for the W_{III} system is given in Table 1 of the main paper. Curves represent the fit of the *T-S* function (Eqs. S1-S4). Plots were offset by a factor of 0.5 to add clarity. Lysozyme (1.5 g/L_{aq}) was analyzed via the GP-SANS, while all others were analyzed via Bio-SANS.

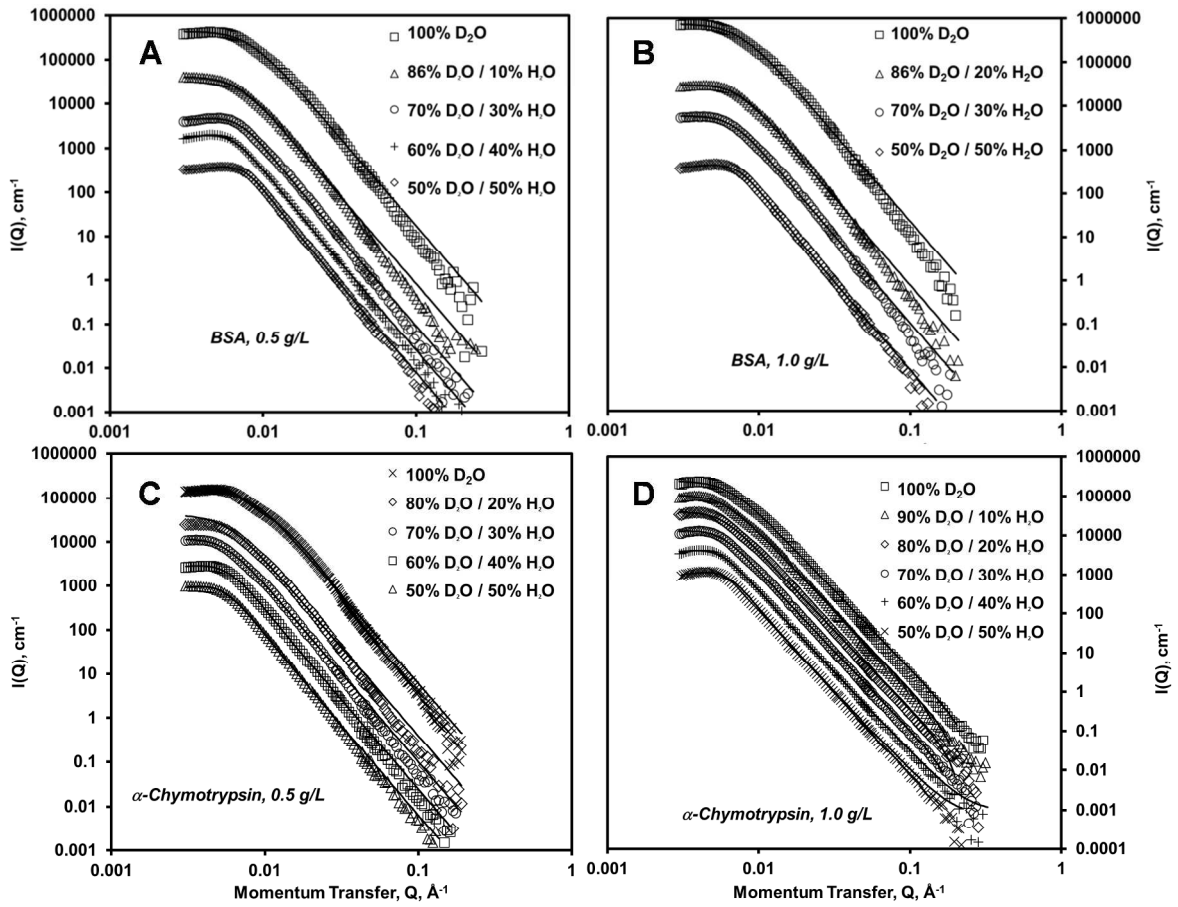

Figure S5. SANS data for the BμE phase of the H_2O+D_2O /AOT /CK2,13-$E_{5.6}$ /Heptane Winsor-III (W_{III}) bicontinuous microemulsion ($B\mu E$) phase at 25°C (*System 2a*; bulk contrast), containing **(A,B)** bovine serum albumin (BSA) and **(C,D)** α-chymotrypsin at 0.5 and 1.0 g/L_{aq} as a function of the H_2O / D_2O ratio. Compositional information for the W_{III} system is given in Table 1 of the main paper. Curves represent the fit of the *T-S* function (Eqs. S1-S4). Plots were offset by a factor of 0.5 to add clarity. α-Chymotrypsin (1.0 g/L_{aq}) samples were analyzed via the GP-SANS apparatus, while all others were analyzed via Bio-SANS.

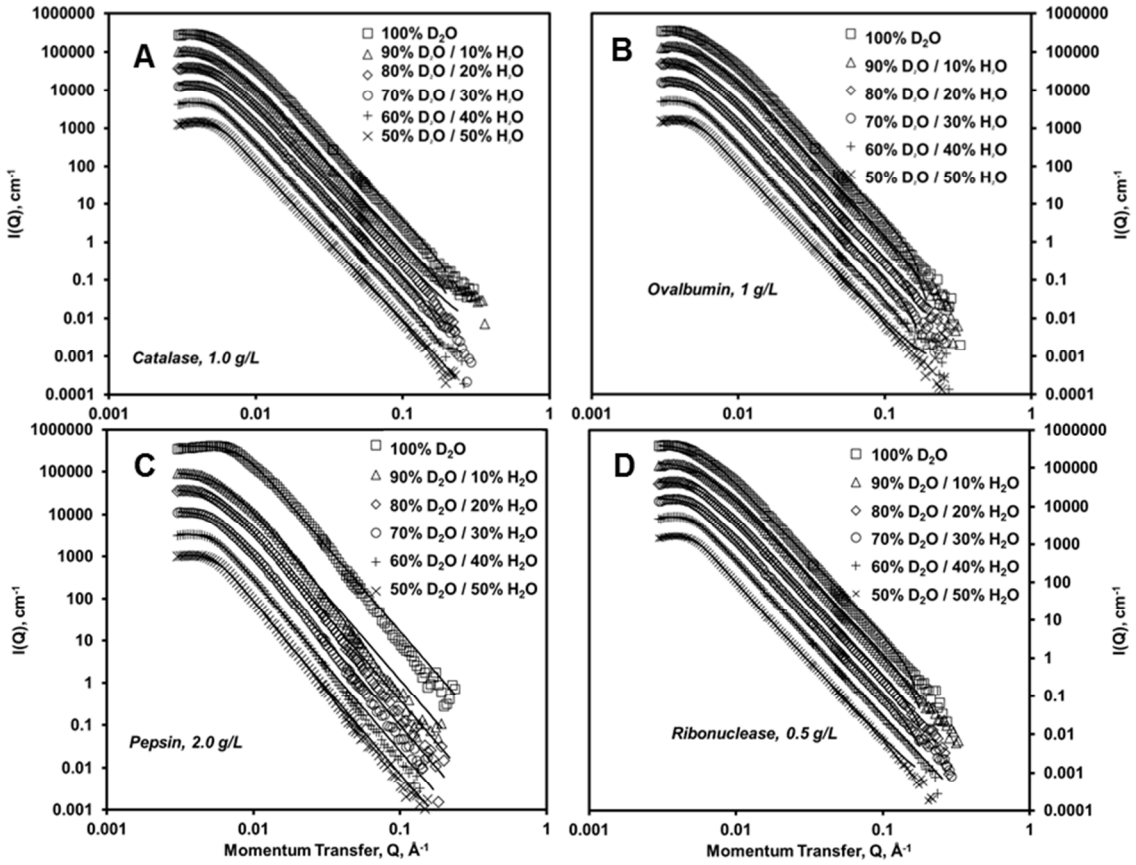

Figure S6. SANS data for the BμE phase of the H_2O+D_2O /AOT /CK2,13-$E_{5.6}$ /Heptane Winsor-III (W_{III}) bicontinuous microemulsion ($B\mu E$) phase at 25°C (*System 2a*; bulk contrast), **(A)** catalase (2.0 g/L_{aq}), **(B)** ovalbumin (1.0 g/L_{aq}), **(C)** pepsin (2.0 g/L_{aq}), and **(D)** ribonuclease (0.5 g/L_{aq}) as a function of the H_2O / D_2O ratio. Compositional information for the W_{III} system is given in Table 1 of the main paper. Curves represent the fit of the *T-S* function (Eqs. S1-S4). Plots were offset by a factor of 0.5 to add clarity. Pepsin (2.0 g/L_{aq}) samples were analyzed via the Bio-SANS apparatus, while all others were analyzed via GP-SANS.

Table S2. Effect of proteins on the surface area per volume (*S/V*) calculated by two different approaches, and monolayer dynamics for the middle, bicontinuous microemulsion, phase of Water/AOT/CK-2,13-$E_{5.6}$/Heptane (*System 2a*), 25°C (bulk contrast) [1,2]

Protein	$[P]_{aq}$, g L^{-1}	κ_{SANS}/k_BT	κ_{theor}/k_BT	S/V_{Porod}, $Å^{-1}$ x 10^3 [3]	$S/V(\xi)$, $Å^{-1}$ x 10^3
No Protein		0.272±0.006	1.28±0.20	1.74±0.14	2.07±0.21
Bovine Serum Albumin	1	0.272±0.026	1.20±0.22	3.46±0.62	2.83±0.29
Bovine Serum Albumin	0.5	0.283±0.033	1.22±0.23	1.82±0.80	2.62±0.29
Catalase	1	0.256±0.007	1.26±0.20	2.29±0.23	2.28±0.23
α-Chymotrypsin	1	0.327±0.009	1.29±0.20	2.10±0.11	2.10±0.21
α-Chymotrypsin	0.5	0.285±0.004	1.27±0.20	0.88±0.09	2.20±0.22
Cytochrome C	1.5	0.454±0.031	1.28±0.21	3.43±0.37	2.54±0.27
Cytochrome C	1	0.403±0.016	1.24±0.20	3.61±0.50	2.78±0.29
Cytochrome C	0.5	0.284±0.010	1.25±0.20	2.06±0.29	2.38±0.25
Lysozyme	1.5	0.623±0.023	1.39±0.20	2.40±0.68	2.36±0.25
Lysozyme	1	0.264±0.014	1.28±0.20	2.49±0.49	2.20±0.27
Lysozyme	0.5	0.301±0.010	1.30±0.20	1.72±0.13	1.97±0.20
Ovalbumin	1	0.278±0.010	1.28±0.20	1.58±0.28	2.11±0.21
Pepsin	2	0.287±0.003	1.27±0.20	2.00±0.48	2.21±0.22
Ribonuclease	0.5	0.276±0.010	1.28±0.20	1.50±0.24	2.07±0.22

[1] Compositional information for the Winsor-III system is given in Table 1 of main paper; [2] Column headings: $[P]_{aq}$ = concentration of protein in aqueous solutions used to form W_{III} system; κ_{SANS}: normalized bending modulus (Eq. S6), k_B: Boltzmann's constant, T: absolute temperature, κ_{theor}: theoretical bare bending elasticity constant (Eq. S8), S/V_{Porod} and $S/V(\xi)$: surface area per volume (Porod analysis, Eqs. S11 and S13) and via ξ (Eq. S5), respectively, [3] determined by plotting apparent SANS-derived values versus $(\Delta\rho)^2$, and extrapolating to $(\Delta\rho)^2=0$ (Figures 3, S3, S4, and S8), with errors reflecting uncertainty from linear regression fitting of the plots.

As shown in Table S2, there is good agreement between the two different estimates of *S/V*, thereby validating the main approach used to determine *S/V* (shown in Figures 3D and S7). In addition, proteins produced only minor changes in κ_{theor}.

Determination of S/V$_{Porod}$

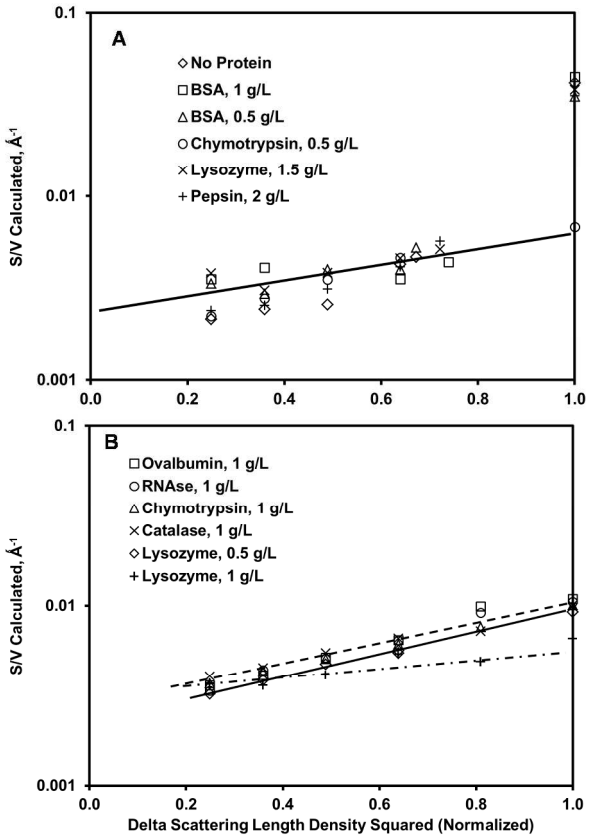

Figure S7. Effect of scattering length density squared, $(\Delta\rho)^2$, on the surface area per volume, *S/V*, derived via a modified Porod law (Eqs. S11 and S13), from SANS data for the H_2O+D_2O/AOT/CK2,13-$E_{5.6}$/Heptane Winsor-III (W_{III}) bicontinuous microemulsion ($B\mu E$) phase at 25°C (*System 2a*; bulk contrast). Compositional information for the W_{III} system is given in Table 1 of the main paper. Data was obtained using the **(A)** Bio-SANS and **(B)** GP-SANS apparatus at ORNL, respectively. Values of *S/V* were obtained by extrapolating to $(\Delta\rho)^2$=0, to minimize the effect of multiple scattering.

Evaluation of the Porod invariant

To confirm that multiple scattering did not affect the reliability of the Porod analysis in the limit as $Q \rightarrow 0$, and that a sharp interface separated the *BμEs*' surfactant monolayers and the nanochannels, the Porod invariant, $\overline{Q}_{\exp}$, was calculated from experimental data:

$$\overline{Q}_{\exp} = \int_0^{\infty} I(Q) Q^2 dQ \qquad \text{(S15)}$$

and compared to a theoretical estimate, $\overline{Q}_{theor}$

$$\overline{Q}_{theor} = 2\pi^2 \phi_{w,mid} \left(1 - \phi_{w,mid}\right) \left(\Delta\rho\right)^2 \qquad \text{(S16)}$$

where $\phi_{w,mid}$ is the volume fraction of water in the middle (*BμE*) phase and $(\Delta\rho)^2$ is the scattering length density difference squared, between the aqueous and oil subphases. Agreement between the two estimates of the Porod invariant (i.e., $\overline{Q}_{\exp} \approx \overline{Q}_{theor}$) would confirm the reliability of the Porod data. Results, given in Table S3 and Figure S8 for two different systems, clearly demonstrate that multiple scattering produces a value of $\overline{Q}_{\exp}$ that is significantly larger than $\overline{Q}_{theor}$. However, in the limit as $(\Delta\rho)^2 \rightarrow 0$, $\overline{Q}_{\exp} / \overline{Q}_{theor} \rightarrow 1$. Therefore, the treatment of the Porod data, i.e., the determination of S/V_{Porod} by plotting apparent S/V_{Porod} values vs. $(\Delta\rho)^2$, and extrapolating to $(\Delta\rho)^2 = 0$, is appropriate. The comparison of $\overline{Q}_{\exp}$ and $\overline{Q}_{theor}$ was also performed for a representative sample of the AOT/CK-2,13-$E_{5.6}$ + -E_3 system. As shown in Table S4, $\overline{Q}_{\exp} / \overline{Q}_{theor} > 2$, suggesting that multiple scattering provides an overestimation of S/V_{Porod}.

Table S3. Evaluation difference between experimental and theoretical values of the Porod invariant ($\overline{Q}_{\exp}$ and $\overline{Q}_{theor}$) for representative bicontinuous microemulsion ($B\mu E$) systems [1]

$B\mu E$ / W_{III} System	Protein	SANS Instrument	Vol. Fract. D_2O in Water	$\overline{Q}_{\exp}$ / $\overline{Q}_{theor}$ [1]
AOT/CK-2,13-$E_{5.6}$	Cytochrome C, 1.5 g/L_{aq}	Bio-SANS	1.0	1.91
AOT/CK-2,13-$E_{5.6}$	Cytochrome C, 1.5 g/L_{aq}	Bio-SANS	0.9	1.50
AOT/CK-2,13-$E_{5.6}$	Cytochrome C, 1.5 g/L_{aq}	Bio-SANS	0.8	1.45
AOT/CK-2,13-$E_{5.6}$	Cytochrome C, 1.5 g/L_{aq}	Bio-SANS	0.7	1.18
AOT/CK-2,13-$E_{5.6}$	Cytochrome C, 1.5 g/L_{aq}	Bio-SANS	0.6	1.30
AOT/CK-2,13-$E_{5.6}$	Cytochrome C, 1.5 g/L_{aq}	Bio-SANS	0.5	0.92
AOT/CK-2,13-$E_{5.6}$	Catalase, 1.0 g/L_{aq}	GP-SANS	1.0	2.91
AOT/CK-2,13-$E_{5.6}$	Catalase, 1.0 g/L_{aq}	GP-SANS	0.9	2.22
AOT/CK-2,13-$E_{5.6}$	Catalase, 1.0 g/L_{aq}	GP-SANS	0.8	1.98
AOT/CK-2,13-$E_{5.6}$	Catalase, 1.0 g/L_{aq}	GP-SANS	0.7	1.79
AOT/CK-2,13-$E_{5.6}$	Catalase, 1.0 g/L_{aq}	GP-SANS	0.6	1.55
AOT/CK-2,13-$E_{5.6}$	Catalase, 1.0 g/L_{aq}	GP-SANS	0.5	1.39
AOT/CK-2,13-$E_{5.6+3}$	Cytochrome C, 1.0 g/L_{aq}	NIST-NG3	0.0	2.08

[1] calculated via Eqs. S15 and S16

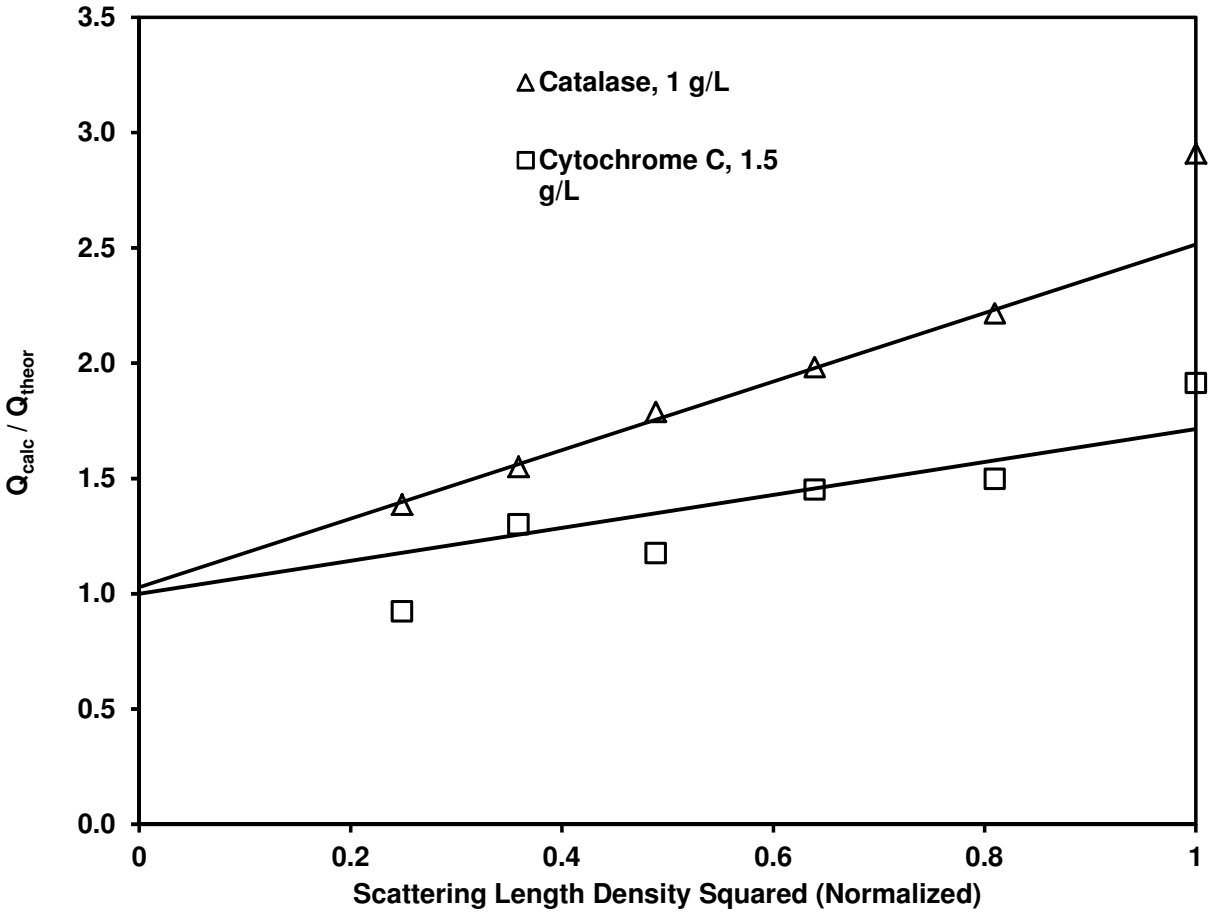

Figure S8: Effect of scattering length density squared on ratio of experimental to theoretical values of the Porod invariant ($\overline{Q}_{\exp}$ and $\overline{Q}_{theor}$). Data was taken from Table S3.

Parameters derived from film contrast SANS data

Table S4. Effect of proteins on SANS modeling for the middle, bicontinuous microemulsion, ($B\mu E$) Winsor-III phase of D_2O/AOT/CK-2,13-$E_{5.6}$/*d*-Heptane (*System 2b*), 25°C (film contrast) [1-3]

Protein	$[P]_{aq}$, g L^{-1}	I_0,cm^{-1} [4]	a_s, $Å^2$ [5]
No Protein	0.0	227±12	270
Bovine Serum Albumin	2.0	371±73	285
α-Chymotrypsin	2.0	326±69	257
Cytochrome C	2.0	123±6	288
Lysozyme	1.3	397±36	299
Pepsin	2.0	246±47	292

[1] Compositional information for the Winsor-III system is given in Table 1 of the main paper; [2] Column headings: $[P]_{aq}$ = concentration of protein in aqueous solutions used to form W_{III} system; I_0 = scattered intensity at $Q=0$ (Eq. S9), a_s = surface area per surfactant (Eq. 1 of main paper); [3] SANS data and fits of Ornstein-Zerneke and modified Porod plot (Eqs. S9 and S12) to the data are given in Figure 4A; [4] error determined by fit of Eq. S9 to SANS data at low Q; [5] error is within ±10%.

References for Supporting Document

1. Glinka, C. J.; Barker, J. G.; Hammouda, B.; Krueger, S.; Moyer, J. J.; Orts, W. J. The 30 M Small-Angle Neutron Scattering Instruments at the National Institute of Standards and Technology. *J. Appl. Crystallogr.* **1998,** *31*, 430-445.
2. Lynn, G. W.; Heller, W.; Urban, V.; Wignall, G. D.; Weiss, K.; Myles, D. A. A. Bio-Sans-a Dedicated Facility for Neutron Structural Biology at Oak Ridge National Laboratory. *Phys. B* **2006,** *385-386*, 880-882.
3. Wignall, G. D.; Littrell, K. C.; Heller, W. T.; Melnichenko, Y. B.; Bailey, K. M.; Lynn, G. W.; Myles, D. A.; Urban, V. S.; Buchanan, M. V.; Selby, D. L.; Butler, P. D. The 40 M General Purpose Small-Angle Neutron Scattering Instrument at Oak Ridge National Laboratory. *J. Appl. Crystallogr.* **2012,** *45*, 990-998.
4. Kline, S. R. Reduction and Analysis of Sans and Usans Data Using Igor Pro. *J. Appl. Crystallogr.* **2006,** *39*, 895-900.
5. Arleth, L.; Pedersen, J. S. Droplet Polydispersity and Shape Fluctuations in Aot [Bis(2-Ethylhexyl)Sulfosuccinate Sodium Salt] Microemulsions Studied by Contrast Variation Small-Angle Neutron Scattering. *Phys. Rev. E: Stat., Nonlinear, Soft Matter Phys.* **2001,** *63*, 061406/1-061406/18.
6. Schubert, K. V.; Strey, R.; Kline, S. R.; Kaler, E. W. Small Angle Neutron Scattering near Lifshitz Lines: Transition from Weakly Structured Mixtures to Microemulsions. *J. Chem. Phys.* **1994,** *101*, 5343-55.
7. Schubert, K. V.; Strey, R. Small-Angle Neutron Scattering from Microemulsions near the Disorder Line in Water/Formamide–Octane-C_ie_j Systems. *J. Chem. Phys.* **1991,** *95*, 8532-8545.
8. Gompper, G.; Endo, H.; Mihailescu, M.; Allgaier, J.; Monkenbusch, M.; Richter, D.; Jakobs, B.; Sottmann, T.; Strey, R. Measuring Bending Rigidity and Spatial Renormalization in Bicontinuous Microemulsions. *Europhys. Lett.* **2001,** *56*, 683.
9. Engelskirchen, S.; Elsner, N.; Sottmann, T.; Strey, R. Triacylglycerol Microemulsions Stabilized by Alkyl Ethoxylate Surfactants—a Basic Study: Phase Behavior, Interfacial Tension and Microstructure. *J. Colloid Interface Sci.* **2007,** *312*, 114-121.
10. Maccarrone, S.; Byelov, D. V.; Auth, T.; Allgaier, J.; Frielinghaus, H.; Gompper, G.; Richter, D. Confinement Effects in Block Copolymer Modified Bicontinuous Microemulsions. *J. Phys. Chem. B* **2013,** *117*, 5623-5632.
11. Holderer, O.; Frielinghaus, H.; Monkenbusch, M.; Klostermann, M.; Sottmann, T.; Richter, D. Experimental Determination of Bending Rigidity and Saddle Splay Modulus in Bicontinuous Microemulsions. *Soft Matter* **2013,** *9*, 2308-2313.